Cocrystallization Behavior of Poly(3-alkylthiophenes): Influence of Alkyl Chain Length and Head to Tail Regioregularity

Susmita Pal and Arun K. Nandi*

Polymer Science Unit, Indian Association for the Cultivation of Science, Jadavpur, Kolkata-700032, India

Received May 26, 2003; Revised Manuscript Received August 16, 2003

ABSTRACT: The cocrystallization behavior of poly(3-alkylthiophene)s (P3ATs) of varying regioregularity and alkyl chain length was explored via differential scanning calorimetry (DSC) and wide-angle X-ray scattering (WAXS) studies. For the regioregular samples both DSC and WAXS studies revealed that cocrystallization was limited to the difference of the alkyl chain length by two carbon atoms. On the other hand, P3AT samples with the same alkyl chain length but different regioregularities cocrystallized with a difference of 17 mol % head to tail (H−T) regularity studied here. P3AT samples with varying regioregularity and alkyl chain length by two carbon atoms showed cocrystallization for a regioregularity difference of 7 mol %. The WAXS study indicated that cocrystals had crystallized within the same interchain lamella and noncocrystals had crystallized within the independent interchain lamella of the components. It also indicated the formation of type 1 P3AT crystals with a noninterdigited side chain during the cocrystallization by melt-quenched conditions for all the samples. The phase diagrams clearly revealed that in some systems at the lower melting component rich region there exist two phase regions. The conductivity of the cocrystals, in both the doped and undoped states, is either intermediate or lower than the line joining their component conductivity values.

Introduction

Poly(3-alkylthiophene)s (P3ATs) are important conducting polymers because of their excellent electrical conductivity, electroluminescence, and nonlinear optical properties.[1] They are reversibly fusible, soluble in organic solvents, and easily processible.[2] These polymers can be produced with different alkyl chain lengths and also with different regioregularities (70−95%).[3−5] Thus, a wide variety of P3ATs with different side chain lengths and different regioregularities are possible, and their physical and conducting properties may depend on the structure of the individual polymers.[5−7] All the P3ATs are semicrystalline in nature,[2,6] and crystallization properties also depend on the side chain length and regioregularity of the samples.[2,5,6] In this paper we present a study on the possibility of cocrystallization between the P3ATs of different alkyl chain lengths and of different regioregularities with an aim to produce polymers with diverse properties without going to the more laborious synthesis of the individual polymers with specific properties.

The cocrystallization in polymers is a difficult proposition, and only a few pairs have been reported to cocrystallize.[8−16] The three important requirements for cocrystallization are (1) structural similarity, (2) similar potential energies, and (3) almost similar crystallization kinetics.[15] The first criterion renders the two polymers miscible in the melt state as well as in the crystalline state. The second requirement justifies that the potential energy of the component chains should be similar for cocrystallization in a common lattice. The last requirement delineates that the crystallization process of the two components should not be much different; a significant difference in rate may induce the two polymers to crystallize separately even if they satisfy the first two conditions. It is very difficult to acquire polymer pairs fulfilling all the above conditions simultaneously, and that is a possible reason only a few cocrystal pairs have been reported in the literature.

The regioregular P3ATs usually have almost the same regioregularity (∼90%) but different alkyl chain lengths which may be varied by a minimum of two carbon atoms. The regioregularity of the polymer can also be changed by applying different polymerization conditions, e.g., polymerization temperature, monomer concentration, etc.[3−5,17] So P3AT chains with similar structures and with similar potential energies may be achieved. In such cases the crystallization kinetics is expected to be similar, yielding a possibility for cocrystallization of the P3AT samples.

P3ATs are comblike polymers and have interchain lamellar structure in the solid state.[18,19] So during the cocrystallization of this new type of polymers the components should have not only a common unit cell but also a common interchain lamella. Now it is established that the side chains of P3ATs also crystallize separately from the main chain. So cocrystallization of the main chain may or may not promote the side chains to cocrystallize and vice versa. Thus, cocrystallization in this system is a complex phenomenon, and in this paper we try to shed light on this complex process. We have used the differential scanning calorimetry (DSC) technique together with wide-angle X-ray diffraction to solve the problem. Also the conductivities of some of the cocrystals were measured to understand how the conductivity of the system changes with cocrystallization.

Experimental Section

A. Samples. Two different groups of P3AT samples, regioregular and regioirregular, were used in the work. The regioregular P3ATs (R = $-C_6H_{13}$, $-C_8H_{17}$, $-C_{12}H_{25}$) were purchased from Aldrich Chemical Co. As reported by the company the samples were prepared by the method of Reike et al.[5] They were purified from the suspended impurities by

* To whom correspondence should be addressed. E-mail: psuakn@mahendra.iacs.res.in.

10.1021/ma034702v CCC: $25.00 © 2003 American Chemical Society
Published on Web 09/27/2003

Table 1. Characteristics of the Samples

P3AT sample	source	$\bar{M}_w \times 10^{-4}$	H−T regioregularity	melting point (°C)
P3HT(R)	Aldrich	8.7	92	222
P3OT(R)	Aldrich	14.2	89	164
P3DDT(R)	Aldrich	16.2	87	120, 134
P3HT-1	prepared	8.7	75	161
P3HT-2	prepared	10.6	82	182

filtering their solution in chloroform and were then dried at 60 °C in a pull of air and finally in a vacuum at 60 °C for 3 days. The head to tail (H−T) regioregularities of the samples were measured from their ^{1}H NMR spectra in a Bruker 300 MHz instrument using the peaks of the α carbon of the 3-substituted thiophene. For the synthesis of regioirregular poly(3-hexylthiophene), the monomer 3-hexylthiophene was synthesized from 3-bromothiophene and *n*-hexyl bromide using a Grignard reaction. It was purified by passing its petroleum ether solution through a silica gel column. The polymer was synthesized in $CHCl_3$ medium using anhydrous $FeCl_3$ as initiator under a nitrogen atmosphere.[17] The polymerization temperature was +2 °C for the first set and −5 °C for the second set of experiments. The reaction was carried out for 24 h, and the reaction mixture was poured into methanol containing 10% HCl. The precipitate was collected, washed with methanol, and dissolved in $CHCl_3$. It was again filtered, and the solution was dried in a pull of air and finally in a vacuum at 60 °C for 3 days. The molecular weights of the prepared samples were measured from gel permeation chromatography (Waters) using a μ-styragel column in tetrahydrofuran at 30 °C. Polystyrene samples were used as standards. The characteristics of the samples are presented in Table 1.

Blends were prepared by dissolving the two-component polymers in different proportions in distilled chloroform and then evaporating to dryness in a pull of air and finally in a vacuum at 60 °C for 3 days.

B. Differential Scanning Calorimetry. A Perkin-Elmer DSC-7 fitted with intracooler-1 and working under a nitrogen atmosphere was used in the work. The instrument was calibrated with indium before each set of experiments. About 3 mg samples were placed in aluminum pans, and the pans were sealed. The samples were melted at a temperature ~30 °C higher than the melting point of the higher melting component (Table 1) for 5 min and were then quenched to −30 °C. After equilibration for 10 min, they were then heated at a rate of 20 °C/min from −30 °C to the above melting temperature. The endotherms were recorded, and the peak temperatures and enthalpy of fusion were measured using the computer attached to the instrument. The cooling thermograms of the samples were also recorded by cooling from the same melting temperature at a rate of 5 °C/min. The crystallization temperature and enthalpies of crystallization were also recorded from the computer attached to the instrument.

C. Wide-Angle X-ray Scattering (WAXS). The WAXS experiments were done on melt-quenched films. In a Mettler FP-82 hot stage they were melted at a temperature 15 °C higher than the melting point of the higher melting component and quenched at room temperature (30 °C) under a nitrogen atmosphere in the hot stage. The experiment was carried out in a Seifert X-ray diffractometer (C 3000) with a parallel beam optics attachment. The instrument was operated at a 35 kV voltage and a 30 mA current and was calibrated with a standard silicon sample. The samples were scanned from a $2\theta = 2°$ value at the step scan mode (step size 0.03°, preset time 2 s), and the diffraction pattern was recorded using a scintillation counter detector.

D. dc Conductivity Measurement. The dc conductivities of the samples at 30 °C were measured using a two-probe technique with the help of a constant-current (I) direct source electrometer (Keithley, model 617), and the voltage (V) was measured using a multimeter (Keithley, model 2000). The conductivity was calculated from Ohm's law ($\sigma = lI/aV$), where the thickness of the film (l) was measured at three different positions using a screw gauge and the area (a) was measured.

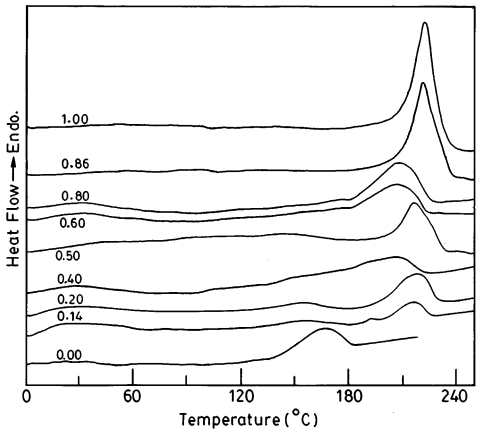

Figure 1. Melting thermograms of the melt-quenched samples of P3HT(R)/P3OT(R) blends at the indicated weight fractions of P3HT(R).

Result and Discussion

A. Thermal Data. 1. Influence of the Side Chain Length. From Table 1 it is clear that the samples have molecular weights ($\bar{M}_w$) in similar ranges; consequently the effect of molecular weight on the cocrystallization process in these systems is considered negligible. In Figure 1 the DSC thermograms of the melting of P3HT(R)/P3OT(R) blends are presented. It is apparent from the figure that the blends have a single melting peak except for the blend compositions $W_{P3OT(R)} = 0.86$ and $W_{P3OT(R)} = 0.80$. These results clearly indicate that the P3HT(R) and P3OT(R) systems produce cocrystals except $W_{P3OT(R)} = 0.86$ and 0.80. The cooling thermograms also corroborate a single crystallization peak for all the compositions except $W_{P3OT(R)} = 0.86$ and 0.80 (Supporting Information Figure 1). It is really an interesting observation as the difference in melting points of the components is quite large (58 °C, Table 1) and still they are forming cocrystals for most of the compositions.

In Figure 2a the DSC thermograms of the blends of P3HT(R)/P3DDT(R) are presented for $W_{P3HT(R)} = 0.60$ and 0.40. The thermograms clearly indicate the presence of component melting peaks denoting the absence of cocrystallization. This is also true for the blends of P3DDT(R)/P3OT(R) (Figure 2b). The melting point difference of the components in the P3HT(R)/P3DDT(R) blend is quite large (~88 °C). So apart from the difference of six carbon atoms in the side chains there may be a large difference in crystallization rate, disfavoring the components to crystallize in a common lattice. Also the potential energy difference of the components may be higher due to a significant difference in the side chain length as for H−H defects in the α polymorph poly(vinylidene fluoride).[20] In the case of P3OT(R)/P3DDT(R) blends the melting point difference (30 °C) is much lower than that of P3HT(R) and P3OT(R), yet they do not cocrystallize. Therefore, it may be argued that in P3OT(R)/P3DDT(R) and P3HT(R)/P3DDT(R) blends both the side chain length difference and their potential energy difference may not fulfill the structural similarity and similar potential energy requirements of cocrystallization mentioned in the Introduction. So from these results it may be surmised that regioregular P3ATs cocrystallize if the difference in side

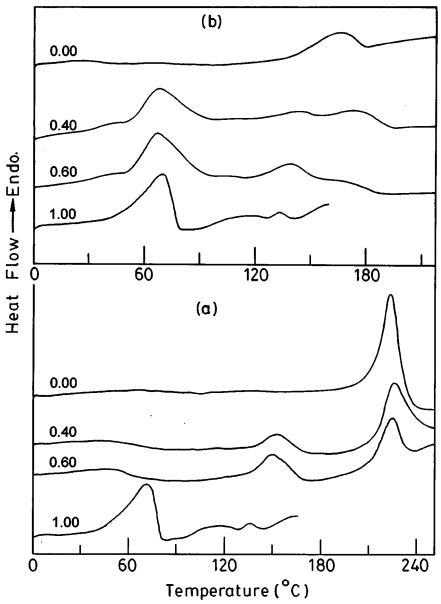

Figure 2. (a) Melting thermograms of the melt-quenched samples of P3HT(R)/P3DDT(R) at the indicated weight fractions of P3DDT(R). (b) Melting thermograms of the melt-quenched samples of P3OT(R)/P3DDT(R) at the indicated weight fractions of P3DDT(R).

chain length is low (e.g., two carbon atoms). However, the reason for the different behavior of the compositions $W_{P3HT(R)} = 0.14$ and 0.20 in P3HT(R)/P3OT(R) blends is yet to be understood.

An important point that needs mention here is the side chain melting peak of P3DDT(R). Pure P3DDT(R) has a sharp side chain melting peak at 70 °C. As P3HT-(R) is added, the peak becomes smaller and broader ($W_{P3HT(R)} = 0.40$), and the peak temperature also decreases with increasing P3HT(R) concentration. With a further increase in the P3HT(R) concentration the side chain melting peak disappears. On the other hand, for the P3OT(R)/P3DDT(R) blends, the side chain melting peak remains as sharp as for pure P3DDT(R) and the melting point decreases with increasing P3OT(R) concentration in the blend. In both the cases the main chains did not exhibit cocrystallization, and a larger difference in the side chain length of the components also disfavored the side chain cocrystallization.

There is a difference in the nature of the P3DDT(R) main chain melting peak compared to those of P3HT-(R) and P3OT(R). The former exhibits two melting peaks, but the latter two exhibit a single peak. The cooling thermogram of P3DDT(R) also exhibits three peaks (Supporting Information Figure 2), two for the main chain and one for the side chain. Different reasons for the two main chain melting peaks of P3DDT(R) are proposed in the literature. Park and Levon[18] considered the lower peak as the melting peak and the higher temperature peak as isotropization of the less ordered phase developed by the restriction of crystallization due to an increase of the sample viscosity. Liu and Chung[21] argued that the lower one is due to melting of the crystalline ordered phase and the higher one is due to melting of the ordered phase produced with the zipping effect of the side chain. It should be mentioned here that the two main chain melting peaks of P3DDT(R) merge to a single peak in both the blends, and so do the crystallization peaks (Supporting Information Figure 2). The reason is not yet clear, and perhaps the partial

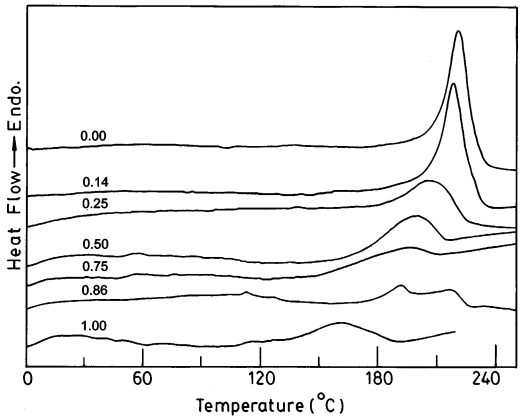

Figure 3. Melting thermograms of the melt-quenched samples of P3HT(R)/P3HT-1 blends at the indicated weight fractions of P3HT-1.

cocrystallization of the components in both the systems yielded the single melting peak.

2. Influence of Regioregularity. In Figure 3 the melting endotherms of P3HT(R) and P3HT-1 characterize the formation of cocrystals for all the compositions except $W_{P3HT-1} = 0.86$. Here the melting point difference of the components is also large (~61 °C) corresponding to a H−T regioregularity difference of 17 mol %, yet they produce cocrystals covering the major region of the concentration spectrum. The components have the same side chain length, but the H−T regioregularities differ significantly. In analogy with the influence of H−T regioregularity on the potential energy of a poly-(vinyledene fluoride) (PVF_2) chain,[20] the potential energy of a P3AT chain may also depend on the H−T regioregularity. The larger the difference in H−T concentration in P3ATs the larger the difference in potential energy if the conformational characteristics remain the same. This system, despite the above large difference in regioregularity, cocrystallizes, whereas in poly-(vinylidene fluoride) samples the difference was limited to a 12 mol % H−H defect concentration under melt-quenched conditions.[15] Thus, it may be argued that either the potential energy variation in P3ATs with H−T regioregularity is less than that in PVF_2 or the P3AT unit cell can tolerate a greater difference of potential energy than that of PVF_2; the exact cause is not yet known.

Blends of P3HT-2 with P3HT(R) were also studied (Figure 4). Here the difference in regioregularity is only 10 mol %, and the melting point difference is only 40 °C. The melting endotherms of the blends clearly corroborate cocrystallization for all the compositions though there is a broadness in the endothermic peak of the blend with $W_{P3HT-2} = 0.86$. In the P3HT-1 and P3HT-2 blends (difference of regioregularity 7 mol %) cocrystallization was also observed throughout the whole composition range (Figure 5). The cooling thermograms (Supporting Information Figures 4 and 5) also support the cocrystalization in all these systems.

3. Influence of Varying Both the Side Chain Length and Regioregularity. In Figure 6 the endotherms of the melt-quenched blends of P3OT(R) and P3HT-2 are presented, and it is evident from the figure that all the compositions have a single and sharp melting peak. Thus, it is good evidence of cocrystallization despite the samples having both a 7 mol % difference in regioregularity and a difference in side chain length of two carbon atoms. The melting point

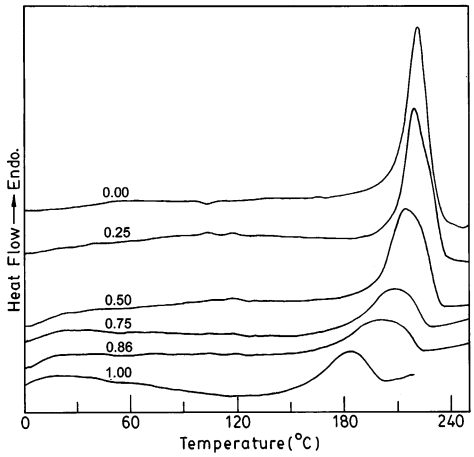

Figure 4. Melting thermograms of the melt-quenched samples of P3HT(R)/P3HT-2 blends at the indicated weight fractions of P3HT-2.

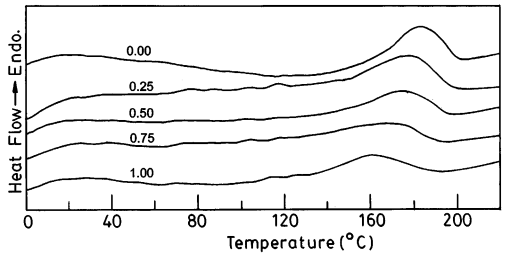

Figure 5. Melting thermograms of the melt-quenched samples of P3HT-1/P3HT-2 blends at the indicated weight fractions of P3HT-1.

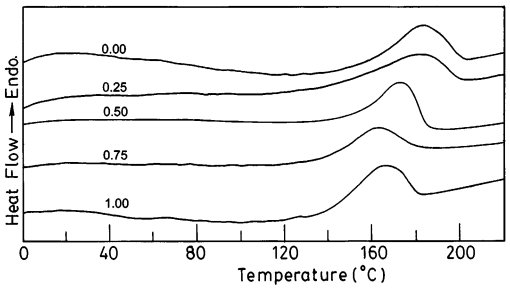

Figure 6. Melting thermograms of the melt-quenched samples of P3HT-2/P3OT(R) blends at the indicated weight fractions of P3OT(R).

difference of the components is very low (18 °C), and it may be a favorable reason for the cocrystal formation despite the variation in both regioregularity and alkyl chain length.

4. Phase Diagram. The phase diagrams of the cocrystals are presented in Figure 7 to visualize the results at a glance. The closed loop structures in the phase diagram are present in P3HT(R)/P3OT(R) and P3HT(R)/P3HT-1 blends. In P3OT(R)/P3HT-2, P3HT-(R)/P3HT-2, and P3HT-1/P3HT-2 blends the phase diagrams are represented by a single line, indicating isomorphic cocrystallization occurred for the whole composition range. The formation of a closed loop structure as in the former two systems is not uncommon during cocrystallization, and it was observed in many other systems. For example, Keller and co-workers[14,22−24] observed that the blends of linear polyethylene (LPE) with branched polyethylene (BPE) did not produce cocrystals at all the compositions, and this has been attributed to the biphasic nature of the melt at BPE-rich compositions. However, Alamo et al.[25] reported from a small angle neutron scattering (SANS) study that the above behavior is due to the difference in crystallization behavior of these compositions. A similar closed loop phase diagram was also observed in the cocrystal system of poly(vinylidene fluoride) and vinylidene fluoride−tetrafluoroethylene copolymers from our laboratory and was attributed to the liquid−liquid phase separation at the melt.[24] The cause of the closed loop structure in the phase diagram of the P3AT blends will be illuminated in a forthcoming paper.

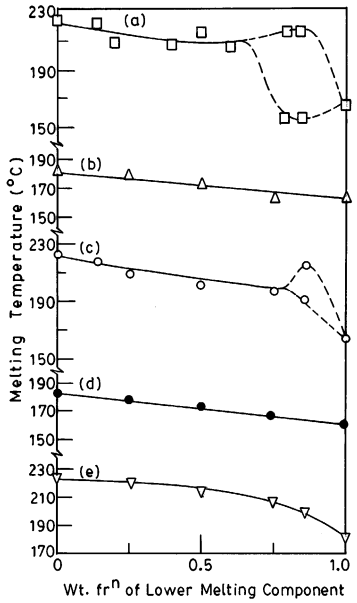

Figure 7. Phase diagram of P3AT cocrystals: (a) P3OT(R)/P3HT(R), (b) P3OT(R)/P3HT-2, (c) P3HT(R)/P3HT-1, (d) P3HT-1/P3HT-2, and (e) P3HT(R)/P3HT-2 blends.

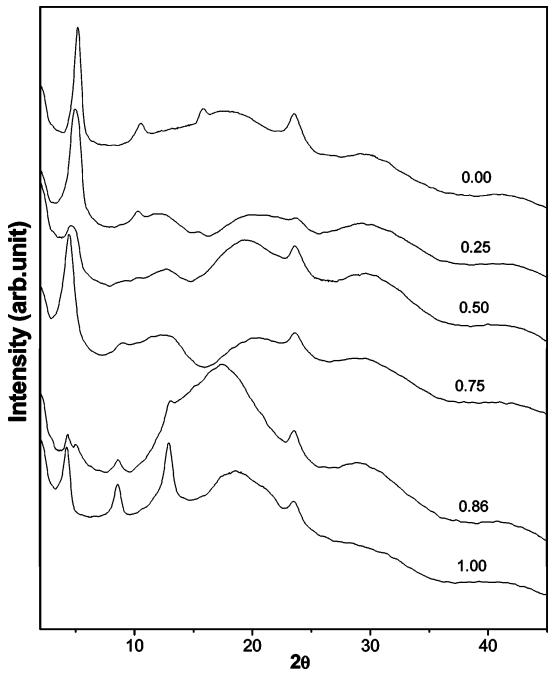

Figure 8. WAXS pattern of P3HT(R)/P3OT(R) blends at the indicated weight fractions of P3OT(R).

B. WAXS Study. To substantiate the above thermal results, a WAXS study of the melt-quenched blends was performed. In Figure 8 the WAXS patterns of P3HT(R) and P3OT(R) blends are presented. Both P3HT(R) and

Table 2. d_{hkl} Values (Å) of P3ATs and Their Blends Produced under Melt-Quenched Conditions

	d_{hkl}[a] at the indicated weight fraction of the lower melting point component														
	P3HT-2 + P3OT(R)					P3HT(R) + P3OT(R)					P3HT(1) + P3HT(R)				
hkl	0.00	0.25	0.50	0.75	1.00	0.00	0.25	0.50	0.75	1.00	0.00	0.25	0.50	0.75	1.00
100	17.07	18.70	20.20	20.10	20.70	16.90	17.40	19.33	20.00	20.70	16.90	17.00	17.00	16.90	
200	8.5			10.60	10.30	8.46	8.60	9.60	9.80	10.30	8.46		8.35	8.40	7.23
		7.14	7.16			6.09	7.30	6.90	7.30	6.85	6.09	7.32		6.90	
300	5.61			7.25	6.85	5.61	5.81				5.61			5.51	
211	4.96				4.79	4.67	4.50	4.63	4.30	4.79	4.67	4.80	4.89	5.09	4.86
301															
		4.24	4.14	4.11											
020		3.76	3.78	3.77	3.78	3.78	3.74	3.78	3.77	3.78	3.78	3.80	3.78	3.86	3.82
510	3.10		3.01	3.08				3.03				3.21	3.22	3.06	
	2.22	2.19	2.19	2.22									2.89	2.19	

[a] d_{hkl} values are assigned according to ref 29.

P3OT(R) have interchain lamellar peaks at 16.9 and 20.7 Å, respectively,[26−29] and they are also present in the blends with an intermediate value of lamellar thickness. The physical interpretation for the blends having a single lamellar peak is that cocrystallization of P3HT(R) and P3OT(R) enables them to crystallize in a common interchain lamella, and the lamellar thickness progressively increases with increasing P3OT(R) in the blend. Again for the composition $W_{P3OT(R)} = 0.86$ there are two interchain lamellar peaks corresponding to 20.2 and 16.9 Å, respectively. Also the amorphous peak at $2\theta = 17.4°$ is larger than that of the other compositions. A probable reason may be the liquid−liquid phase separation at the melt disfavors the crystallization process of this blend, producing a larger amorphous peak. Thus, the X-ray results clearly substantiate the thermal results for cocrystallization in this system.

The X-ray diffraction peak positions of the blends are presented in Table 2. From the table it is apparent that the d_{100}, d_{200}, and d_{300} peaks are present almost in all blends including the pure components. The X-ray diffraction peak at $d_{hkl} = 3.78$ Å is almost invariant in the blends and corresponds to the intrastack chain to chain repeat distance. Another important observation is that a new amorphous peak developed at $2\theta \approx 12°$ in the blends, producing cocrystals. This may arise due to the development of side chain disorder, which usually occurs at ∼13°.[27] In the cocrystals the side chains may not be ordered to the full extent of those in the pure components. So the newly developed amorphous peak at ∼12° may be attributed to the disordering of side chains to some extent during cocrystallization.

In Figure 9 the X-ray diffractrograms of P3HT-1/P3HT(R) blends are presented. It is important to note that P3HT-1 did not show any lamellar structure whereas P3HT(R) and its blends showed lamellar structure with almost the same lamellar distance. Here also the $d_{hkl} \approx 3.8$ Å peak was found to be invariant in all the blends. Thus, it may be inferred from these results that the component not forming an interchain lamellar crystal, however, produces a lameller crystal with the lamellar-forming component. Probable support of this assertion is that the lamellar peaks of the blends were quite sharp and the intensity of the peaks did not decrease significantly with increasing P3HT-1. However, the reason for the lack of formation of the interchain lamellar crystal in P3HT-1 is not known; a greater amount of regioregularity in the main chain might hinder the interdigitation of the side chains to form the lamella. The effect of regioirregularity on the side chain amorphous peak at 12.2° is clearly observed for the

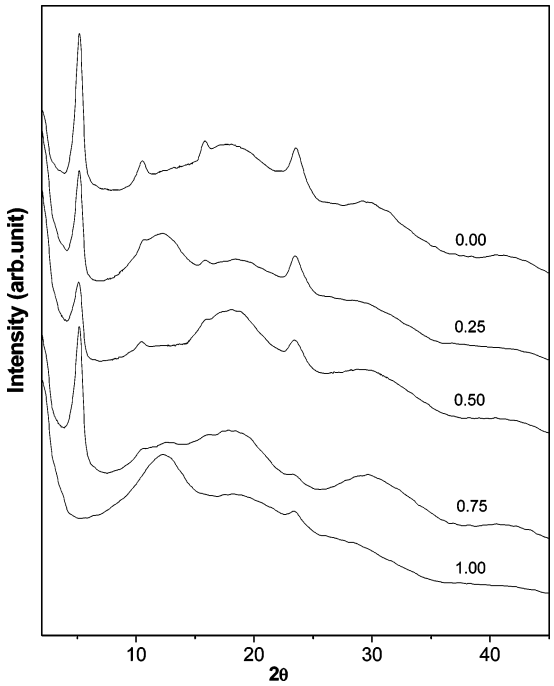

Figure 9. WAXS pattern of P3HT-1/P3HT(R) blends at the indicated weight fractions of P3HT-1.

P3HT-1 sample and is almost absent in the P3HT(R) sample. An addition of 25% (w/w) P3HT-1 disturbs to some extent the side chain ordering of P3HT(R) and produces a side chain amorphous halo. However, the absence of this halo in $W_{P3HT-1} = 0.5$ and 0.75 is interesting, but the reason is not known.

The X-ray diffractogram of P3HT-2/P3OT(R) blends (Figure 10) also showed single lamellar peaks in all the blends, confirming the thermal result that all the blend compositions produced cocrystals. The d_{hkl} values of all the blends are also presented in Table 2. Here a gradual increase of lamellar thickness is observed with increasing $W_{P3OT(R)}$ in the blends. The 3.8 Å peak is invariant in all the blends as in earlier cases. Here also a new side chain amorphous peak appears at $2\theta \approx 12°$ in all the blends for the same reason as discussed earlier.

The X-ray diffractograms of P3DDT(R)/P3HT(R) and P3DDT(R)/P3OT(R) blends at a 1:1 composition are presented in Figure 11. In these systems two lamellar peaks of the components are clearly seen. So these systems indicate the absence of cocrystallization of the components, supporting the thermal results. The two lameller peaks of P3DDT(R)/P3OT(R) blends, however, are not clearly resolved as in the P3DDT(R)/P3HT(R)

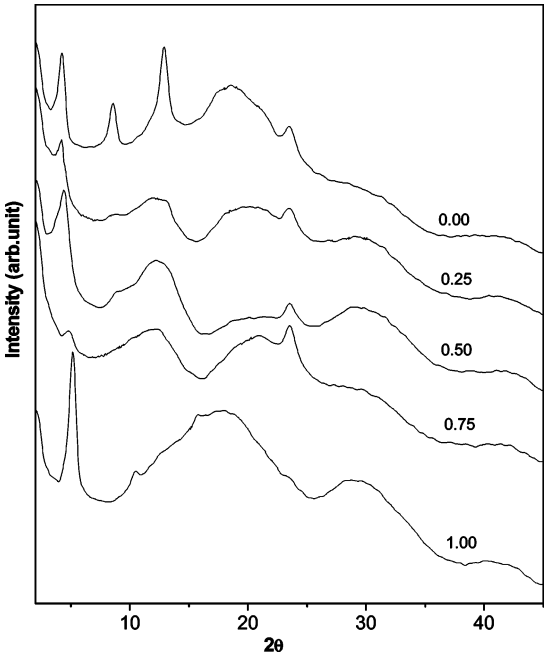

Figure 10. WAXS pattern of P3HT-2/P3OT(R) blends at the indicated weight fractions of P3HT-2.

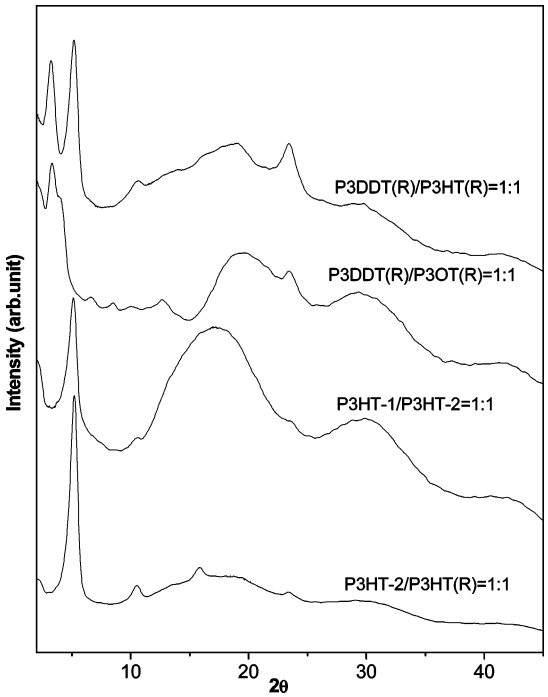

Figure 11. X-ray diffractogram of the indicated blends at their 1:1 composition (by weight).

blends probably because of partial cocrystallization and also because of the lesser difference in d_{100} values of the components than that of the former system. The P3HT-1/P3HT-2 and P3HT-2/P3HT(R) blends showed single lamellar peaks, supporting the thermal results of cocrystal formation. A comparison of the diffractrograms of the latter two systems indicates that in P3HT-2/P3HT(R) the amorphous halo is lower than that of the P3HT-1/P3HT-2 system. This is because of the higher regioirregularity of P3HT-1 than that of P3HT(R). The lamellar peak is sharper in the P3HT-2/P3HT(R) system than in the former one because of the formation of better cocrystals.

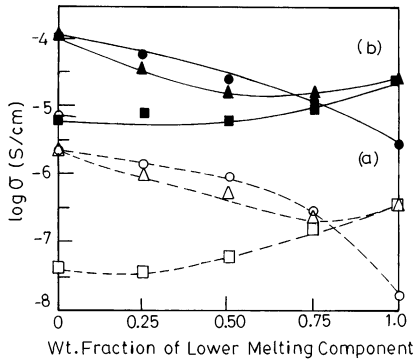

Figure 12. log σ vs composition of the (a) cocrystals and (b) iodine-doped cocrystals: (a) (○) P3HT(R)/P3HT(1); (△) P3HT-(R)/P3OT(R); (□) P3HT(2)/P3OT(R); (b) (●) P3HT(R)/P3HT(1); (▲) P3HT(R)/P3OT(R); (■) P3HT(2)/P3OT(R).

Thus, the X-ray results also conclude that cocrystallization is possible for regioregular P3ATs only with a small difference in the size of the alkyl chains, i.e., by only two carbon atoms. The components crystallized in the same lamella when cocrystallization occurred, but in different lamellae when cocrystallization had not taken place. Again the lamella thickness values and the nature of the X-ray diffractrograms indicated the formation of type 1 crystals in the pure components as well as in the cocrystals produced under the melt-quenched conditions.[27] These type 1 crystals have noninterdigited structure; i.e., the overlap of the side chains in the interlameller stack is minimal, although there is ordering of the side chains across the layer−layer interface.

C. Conductivity. In Figure 12 the room temperature dc conductivities of the undoped and iodine-doped cocrystals are presented. The conductivities of the pure components are close to the value reported in the literature.[5] It is apparent from the figure that the cocrystals, both doped and undoped, have intermediate conductivities for most of the components. In the P3HT-2/P3OT(R) and P3HT(R)/P3OT(R) blends the conductivity passes through a minimum. A probable reason for this decrease in conductivity is that in the cocrystal the lamellar organization is not as perfect as in the pure components and some disorder in the crystal may exist, causing the conductivity to decrease. This assertion is supported by the fact that the X-ray diffractrograms of the cocrystals exhibit an additional side chain amorphous halo which is absent in the pure components, indicating some disorder in the cocrystals. In the P3HT-(R)/P3HT-1 system the components differ only in regioregularity; consequently the decrease is at first linear, and at the P3HT-1-rich region the conductivity rapidly drops to the P3HT-1 value. This, therefore, indicates that by making blends with less costly P3HT-1 we can achieve conductivity close to that of P3HT(R), thereby decreasing the production cost. So it may be concluded from these results that P3AT samples of required conductivity within an approximate good melting range may be prepared by the process of cocrystallization.

Conclusion

The cocrystallization behavior of P3ATs may be summerized as follows: (a) For regioregular samples the cocrystallization is limited to a difference in side chain carbon length of two carbon atoms only. (b) For samples having the same side chain length cocrystallization is possible for a difference in H−T regioregularity of 17 mol % only. (c) For samples with varying side chain

length and regioregularity cocrystallization is possible for a minimum difference in side chain length of two carbon atoms and a difference in H−T regioregularity of 7 mol %. (d) The phase diagram of the cocrystals shows a closed loop structure in the lower melting component rich blend for the P3HT(R)/P3OT(R) and P3HT(R)/P3HT-1 blends. (e) WAXS studies indicate cocrystallization involves single lamellar formation but component lamellas are observed where cocrystallization has not occurred. (f) The interchain lamellar length increases gradually with increasing the longer lamellar component in the blend. (g) The dc conductivity of the cocrystals (both doped and undoped) is intermediate or lower than the intermediate values of the components.

Acknowledgment. We gratefully acknowledge CSIR, New Delhi (Grant No. 1655/00/EMR.11), for financial support.

Supporting Information Available: This material is available free of charge via the Internet at http://pubs.acs.org.

References and Notes

(1) McCullough, R. D.; Ewbank, P. C. In *Handbook of Conducting polymers*, 2nd ed.; Skotheim, T. A., Elsenbaumer, R. L., Renolds, J. R., Eds.; Marcel Dekker: New York, 1998; p 225.
(2) Roncali, J. *Chem. Rev.* **1992**, *92*, 711.
(3) Neimi, V. M.; Knuuttila, P.; Osterholm, J. E.; Korvela, J. *Polymer* **1992**, *33*, 1559.
(4) McCullough, R. D.; Lowe, R. D.; Jayaraman, M.; Anderson, D. *J. Org. Chem.* **1993**, *58*, 904.
(5) Chen, T.-A.; Wu, X.; Rieke, R. D. *J. Am. Chem. Soc.* **1995**, *117*, 233.
(6) Malik, S.; Nandi, A. K. *J. Polym. Sci., Polym. Phys. Ed.* **2002**, *40*, 2073.
(7) Chen, T.-A.; Rieke, R. D. *Synth. Met.* **1993**, *60*, 175.
(8) Natta, G.; Allegra, G.; Bassi, I. W.; Sianesi, D.; Caporiecio, G.; Torti, E. *J. Polym. Sci., Part A: Gen. Pap.* **1965**, *3*, 4263.
(9) Kamiya, H.; Sakuri, M.; Inoue, Y.; Chugo, R. *Macromolecules* **1991**, *24*, 3888.
(10) Hu, S. R.; Kyu, T.; Stein, R. S. *J. Polym. Sci., Polym. Phys. Ed.* **1987**, *25*, 71.
(11) Alamo, R. G.; Glaser, R. H.; Mandelkern, L. *J. Polym. Sci., Polym. Phys Ed.* **1988**, *26*, 2169.
(12) Tanaka, H.; Lovinger, A. J.; Davis, D. D. *J. Polym. Sci.* **1990**, *B28*, 2183.
(13) Tashiro, K.; Izuchi, M.; Kobayashi, M.; Stein, R. S. *Macromolecules* **1994**, *27*, 1221.
(14) Hill, M. J.; Barham, P. J.; Keller, A. *Polymer* **1992**, *33*, 2530.
(15) Datta, J.; Nandi, A. K. *Polymer* **1994**, *35*, 4804.
(16) Guerra, G.; Karasz, F. E.; Macknight, W. J. *Macromolecules* **1986**, *19*, 1935.
(17) Amou, S.; Haba, O.; Shiroto, K.; Hayakawa, T.; Ueda, M.; Takeuchi, K.; Asai, M. *J. Polym. Sci., Polym. Chem.* **1999**, *37*, 1943.
(18) Park, K. C.; Levon, K. *Macromolecules* **1997**, *30*, 3175.
(19) Kim, H. K. Ph.D. Thesis, Polytechnique University, Brooklyn, NY, 1994.
(20) Farmer, B. L.; Hopfinger, A. J.; Lando, J. B. *J. Appl. Phys.* **1972**, *43*, 4293.
(21) Liu, S. L.; Chung, T. S. *Polymer* **2000**, *41*, 2781.
(22) Barham, P. J.; Hill, M. J.; Keller, A.; Rosney, C. C. A. *J. Mater. Sci. Lett.* **1988**, *7*, 1271.
(23) Hill, M. J.; Barham, P. J. *Polymer* **1994**, *35*, 1802.
(24) Datta, J.; Nandi, A. K. *Polymer* **1996**, *37*, 5179.
(25) Alamo, R. G.; Londono, J. D.; Mandelkern, L.; Stehling, F. C.; Wignall, G. D. *Macromolecules* **1994**, *27*, 411.
(26) Tashiro, K.; Kobayashi, M.; Kawai, T.; Yoshino, K. *Polymer* **1997**, *38*, 2867.
(27) Prosa, T. J.; Winokur, M. J. *Macromolecules* **1996**, *29*, 3654.
(28) Prosa, T. J.; Winokur, M. J.; Moulton, J.; Smith, P.; Heeger, A. J. *Macromolecules* **1992**, *25*, 4364.
(29) Tashiro, K.; Ono, K.; Minagawa, Y.; Kobayashi, M.; Kawai, T.; Yoshino, K. *J. Polym. Sci.* **1991**, *B29*, 1223.

MA034702V